New colorimetric rhodamine–helicene "OFF–ON" fluorescence sensor based on FRET for quantitative and qualitative Hg^{2+} determination

Sopida Thavornpradit,[a] Arthorn Loisruangsin,[a] Nirawit Kaewnok,[b] Watthanachai Buaban,[b] Krit Setthakarn,[b] Natdhera Sanmanee,[c] Thanasat Sooksimuang[d] and Nantanit Wanichacheva*[b]

[a]*Division of Chemistry, Department of Physical and Material Sciences, Faculty of Liberal Arts and Science, Kasetsart University, Kamphaeng Saen Campus, Nakhon Pathom, 73140, Thailand*

[b]*Department of Chemistry, Faculty of Science, Silpakorn University, Nakhon Pathom, 73000, Thailand*

[c]*Department of Environmental Science, Faculty of Science, Silpakorn University, Nakhon Pathom, 73000, Thailand*

[d]*National Metal and Materials Technology Center (MTEC), Pathum Thani, 12120, Thailand*

*Corresponding author: E-mail addresses: wanichacheva_n@su.ac.th (N. Wanichacheva)

Table of Contents

1. Characterization data

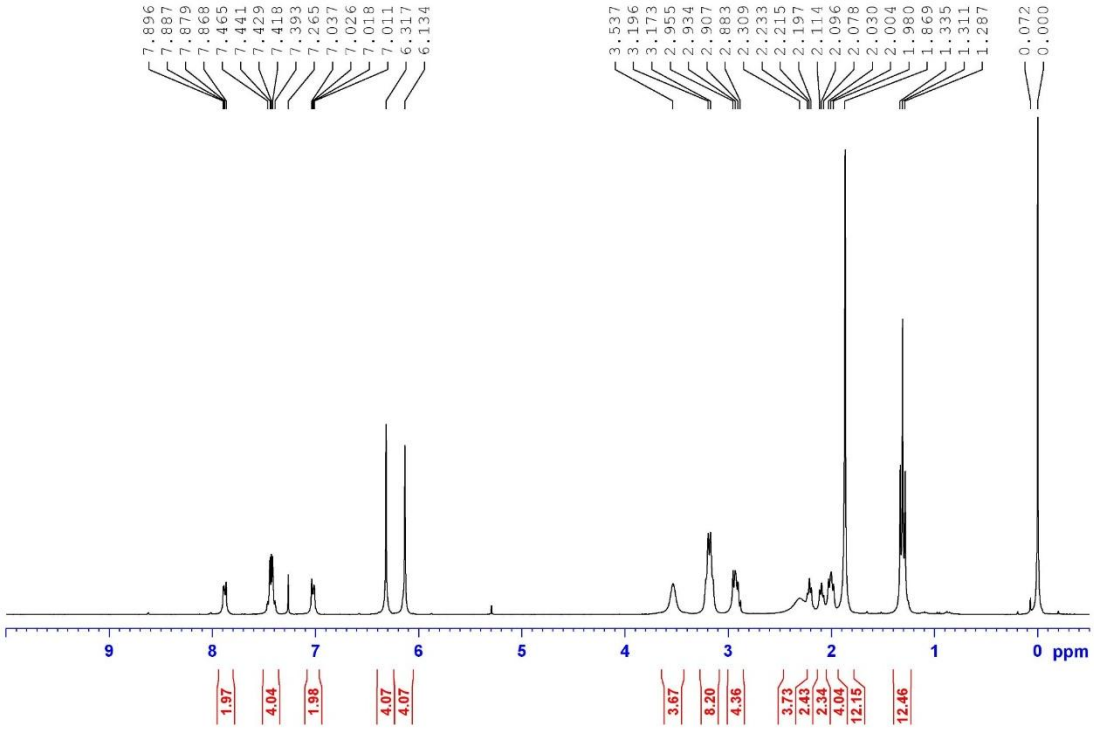

Fig. S1. ^{1}H–NMR of **DG** in $CDCl_3$

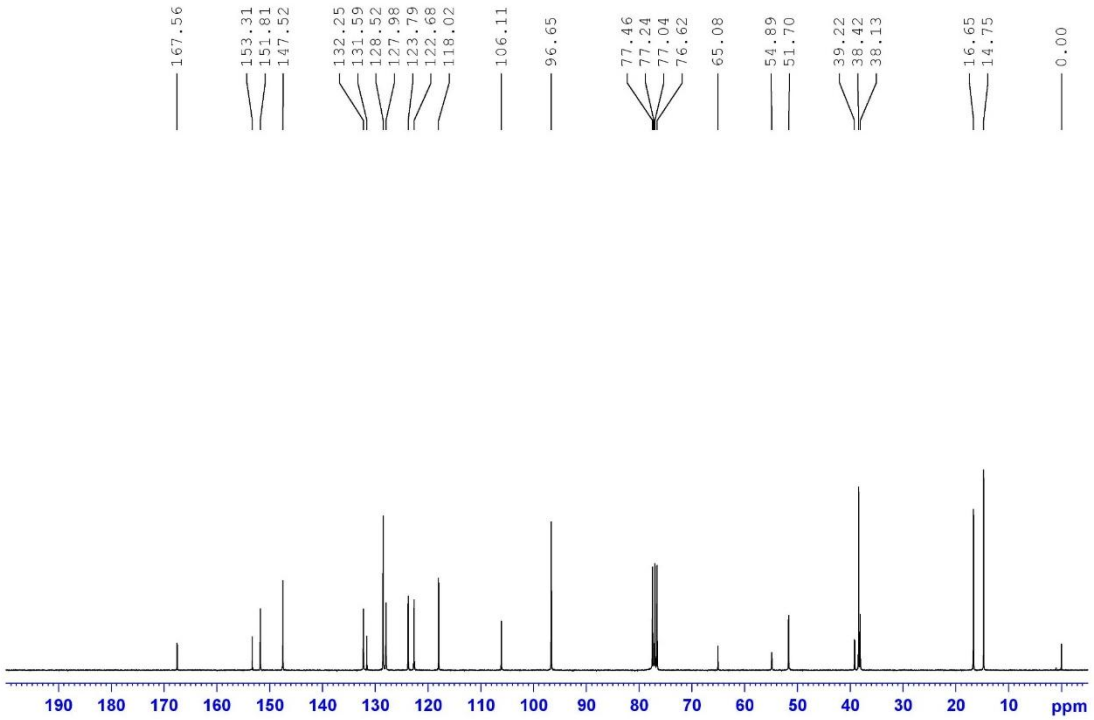

Fig. S2. ^{13}C–NMR of **DG** in $CDCl_3$

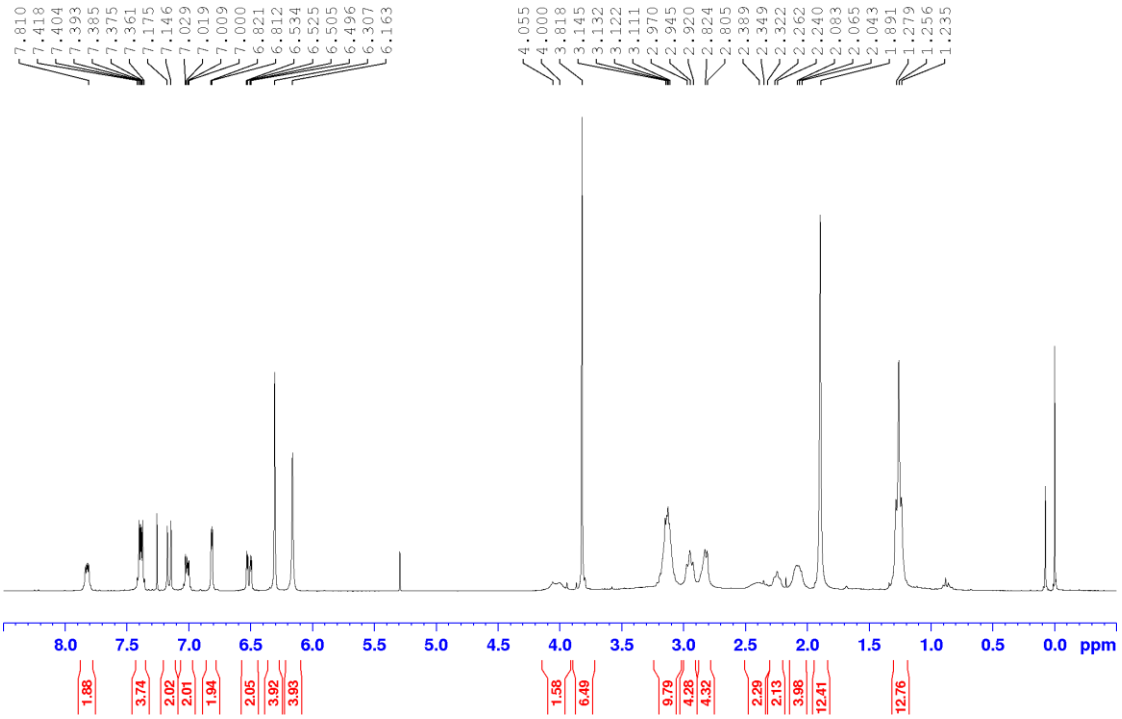

Fig. S3. ^{1}H–NMR of **DGM** in $CDCl_3$

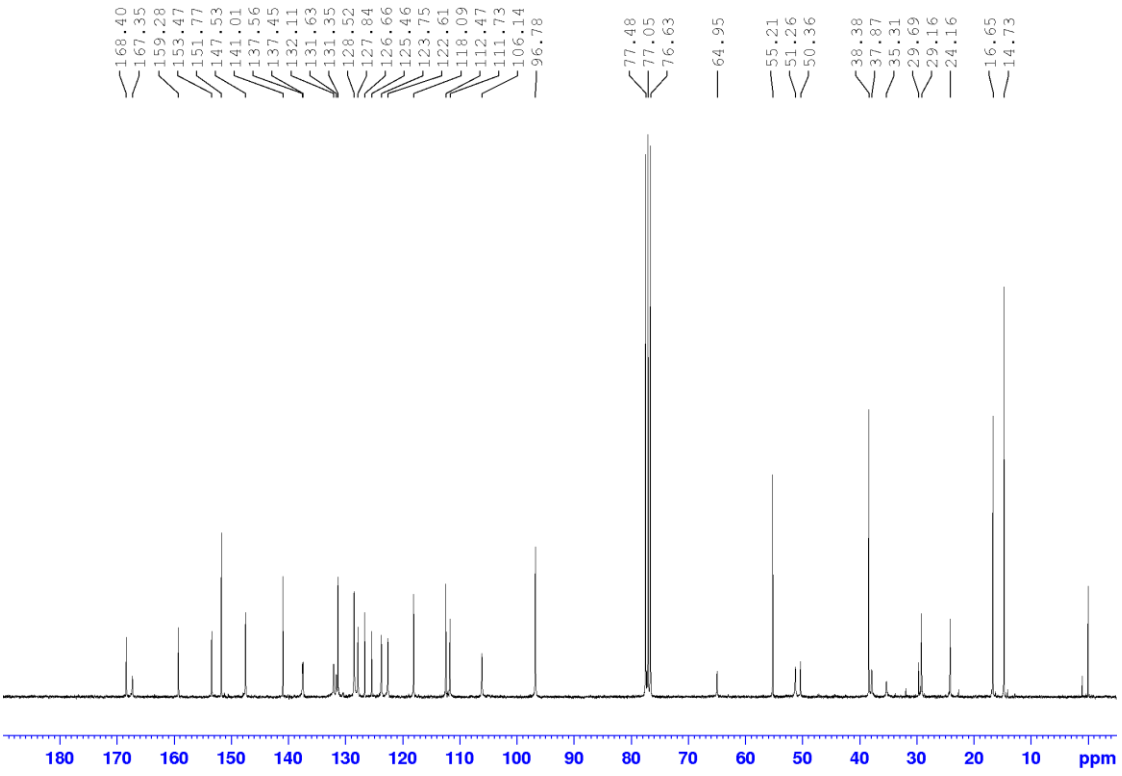

Fig. S4. ^{13}C–NMR of **DGM** in $CDCl_3$

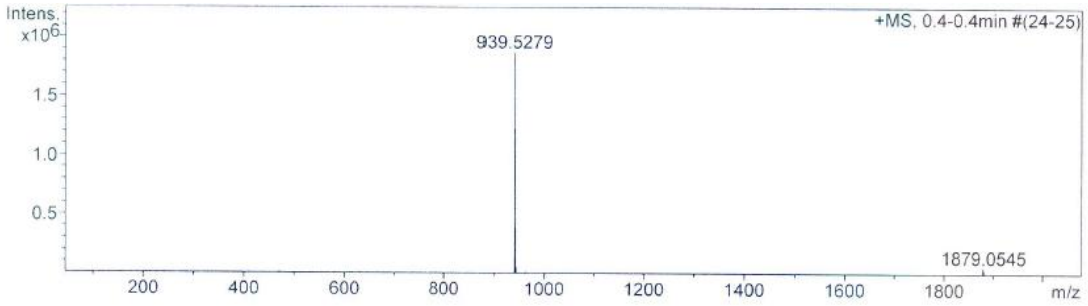

Fig. S5. HRMS of **DG** using MeOH

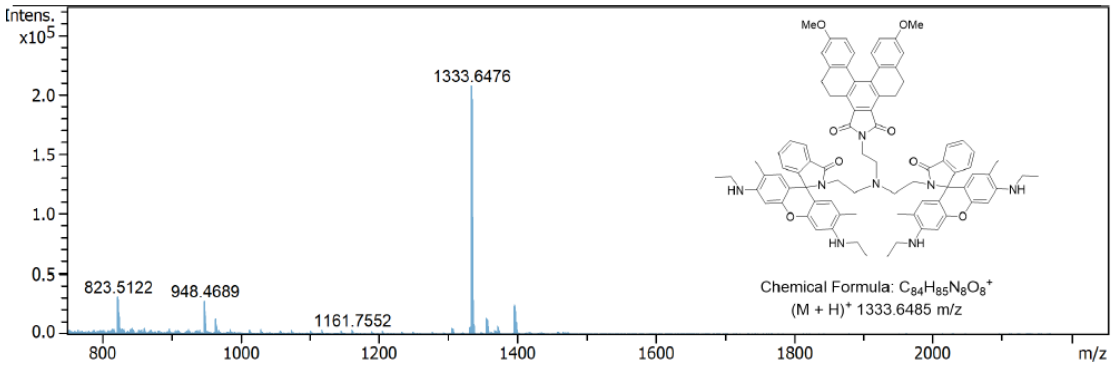

Fig. S6. HRMS of **DGM** using MeOH

2. Absorption and fluorescence emission spectra of DGM

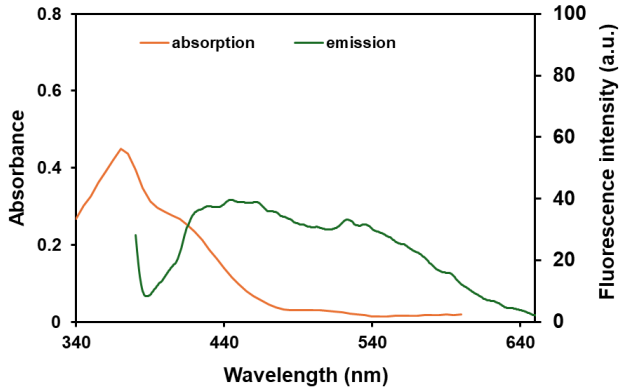

Fig. S7. Absorption and emission spectra (λ_{ex} = 373 nm) of **DGM** in 3%MeOH:H_2O

3. Fluorescence response in three solvent systems

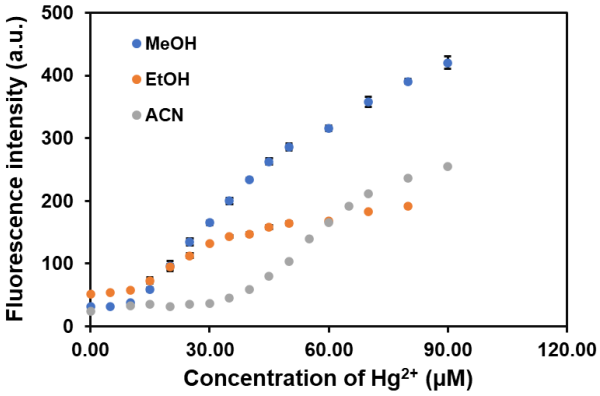

Fig. S8. Fluorescence intensity (λ_{ex} = 373 nm) of **DGM** (6.00 μM) at 549 nm in MeOH, EtOH, and ACN plotted against various concentrations of Hg^{2+}

4. Response time for Hg^{2+} detection

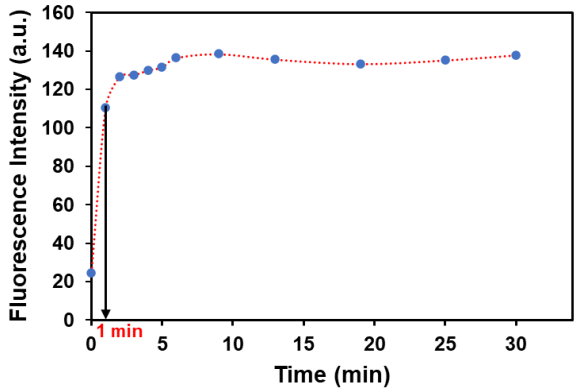

Fig. S9. Fluorescence intensity at 549 nm (λ_{ex} = 373 nm) of **DGM** (6.0 μM) in MeOH:H_2O (97:3) after adding Hg^{2+} (5 eq.) within 30 min

6. Effect of counteranion bound to Hg^{2+}

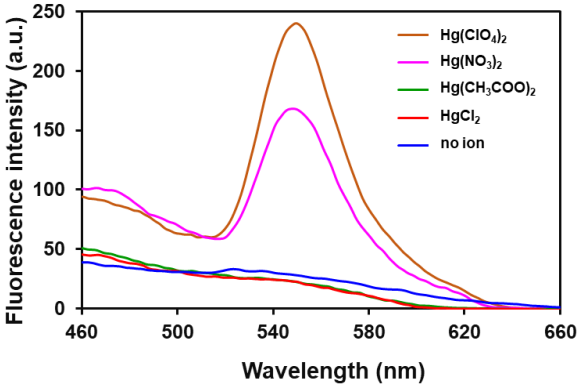

Fig. S10. Emission spectra (λ_{ex} = 373 nm) of **DGM** (6.0 μM) upon the addition of different mercuric salts (5 eq.) in MeOH:H_2O (97:3)

6. Linear range

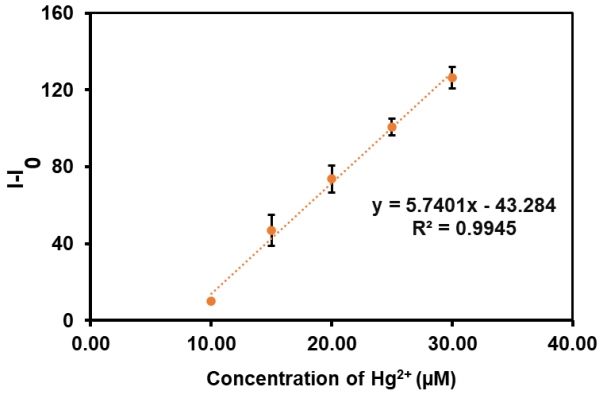

Fig. S11. The linear relation between the fluorescence intensity (λ_{ex} = 373 nm) of **DGM** (6.0 μM) with concentrations of Hg^{2+} (I_0 is the initial fluorescence intensity and I is the fluorescence intensity after the addition of Hg^{2+})

7. pH dependence on Hg^{2+} sensing

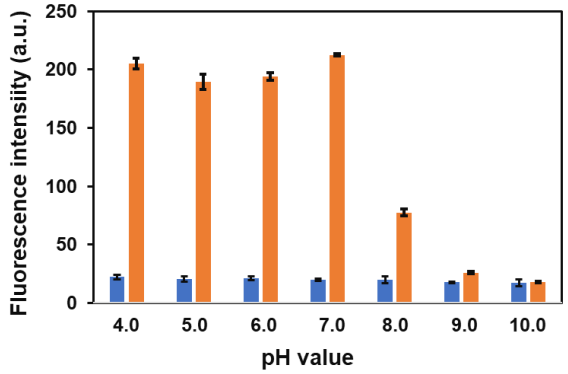

Fig. S12. The fluorescence response (λ_{ex} = 373 nm) of DGM (6.0 μM) in MeOH/HEPES (97:3 v/v, 5.0 mM) with different pH values before adding Hg^{2+} (blue graph) and after adding 10 eq. of Hg^{2+} (orange graph)

8. Benesi-Hildebrand plot

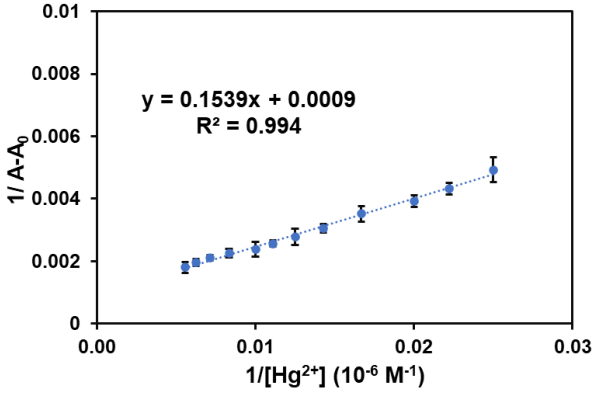

Fig. S13. Benesi–Hilderbrand plot for calculation of K_{assoc} of **DGM**-Hg^{2+}

9. ^{13}C NMR experiment

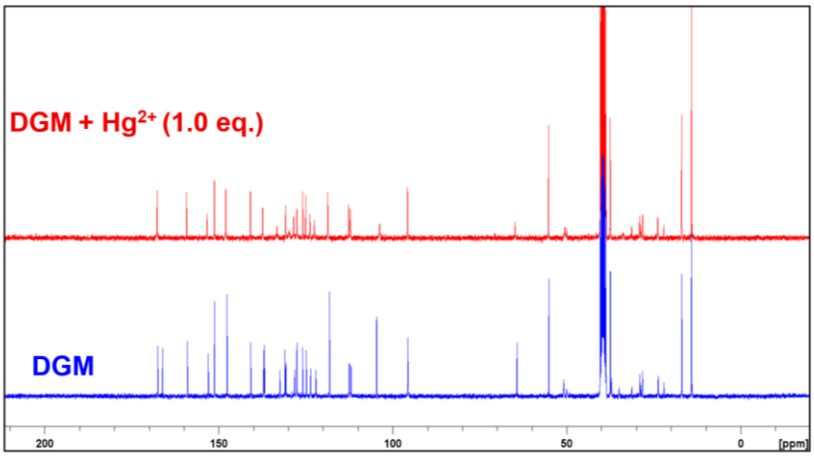

Fig. S14. ^{13}C–NMR spectra of **DGM** in DMSO-d_6 in the absence and presence of Hg^{2+}

10. The selectivity studies by UV-vis spectroscopy

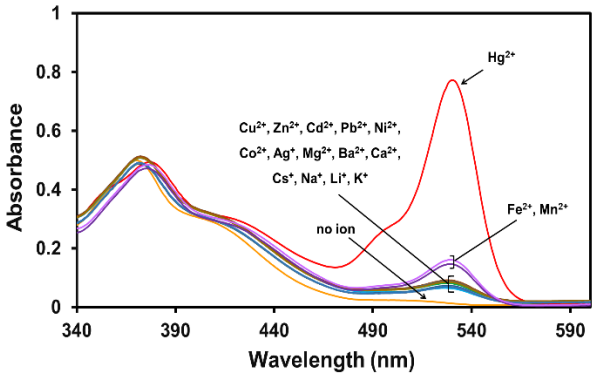

Fig. S15. Absorption spectra of **DGM** (40.00 μM) in 3%H_2O:MeOH with various metal ions (200 μM)